AJNR

Brain tumor CT attenuation coefficients: semiquantitative analysis of histograms.

M Ratzka and I Haubitz

AJNR Am J Neuroradiol 1983, 4 (3) 505-508
http://www.ajnr.org/content/4/3/505

Brain Tumor CT Attenuation Coefficients: Semiquantitative Analysis of Histograms

M. Ratzka[1] and I. Haubitz[2]

This paper reports on work in progress on semiquantitative curve analyses of histograms of brain tumors. Separation of statistical groups of attenuation values obtained by computer calculation is done separately from scanning, using histogram printouts as the data input for a programmable calculator. This method is discussed together with its results in 50 cases of malignant gliomas. The detection of hidden tissue portions and the more accurate evaluation of partial enhancement effects have been the investigators' main concerns to the present time; however, this method may allow more specific diagnosis of malignancy and changes in tumor characteristics than visual assessment alone. This has not been proven by studies that have evaluated large numbers of cases, but seems to be worth pursuing as a new approach.

This paper presents a procedure that enables more effective application of statistical software in CT scanning. Histograms of regions of interest (ROIs) (taken from 50 patients with malignant gliomas) are analyzed in an attempt to make a semiquantitative assessment of the distribution of density values before and after contrast enhancement. The tumors that have been chosen can be classified as glioblastomas or gliomas of grades III and IV, and the histograms of their ROIs form complex curves in a high percentage of the cases. This corresponds to the finding of Kazner et al. [1] that many tumors present with mixed density values.

The possibility of making correct specific (histologic) tumor diagnosis from the CT scan alone is still a matter of controversy. That "everything can look like everything" (Kricheff, cited in [1]) is correct for the single case but must be taken as a postulate—otherwise the appearance of tumors on computed tomography might be considered an unmistakable pathognomonic finding.

But there are always enough cases in which we need additional information. These data may be derived from the histogram curves of tumor ROIs, unless these curves simply represent normal statistical (gaussian) distributions. (In such cases they would provide some information about the mean values of x-ray attenuation coefficients and their standard deviations, which in turn would only indicate that a tumor is hypodense, isodense, or hyperdense compared with normal brain tissue.) Thus we can gain some more inherent information of the tissue type if the histogram does not show a normal distribution pattern.

Materials and Methods

According to the work of Weichselberger [2] and Knoll [3], statistical distributions that differ distinctly from normal distribution patterns that are complex, or that present several peaks, must be assumed to be mixed distributions of two or more normal distributions. Through a series of formulaic and logarithmic transformations, these researchers have reduced distinctly abnormal distributions into a series of practical information packages that can be assessed easily by computer. We have used their methods and formulas in our study to generate the figures of the histogram printout we used. These data are then transfered to punch cards, and these cards are fed into a freely programmable computer (Telefunken TR 440). The calculation consists of graphic elements that can be printed out after any step of the procedure, from the curve of gross values, to gross values in logarithmic scale, to the probability scale, and finally to the integrated curve of the probability scale. Figure 1 shows two very similar approaches to the dissection of a mixed distribution into two normal distributions.

We analyzed the ROIs of 50 CT scans taken from patients with gliomas (grade III–IV) and glioblastomas. All diagnoses were confirmed histologically. We used a scanner model EMI CT 1010 (120 kV, index 240 grades, matrix 160 × 160, thickness of the slices 10 mm). The ROIs were marked by circular or rectangular areas which were placed around the tumors as accurately as possible. All curves were characterized as mixed distributions: either they had several peaks, a widespread standard deviation of the attenuation values, or markedly different steepness of the curve legs.

Results

Histograms without Contrast Enhancement of the Tumors

The ROI histograms could be dissected into two (one case), three (22 cases), four (21 cases), or five (six cases) partial curves. But if we look at the mean values of these dissected normal distributions (partial curves) it is difficult to find a pattern at first.

The next step is to establish groupings based on mean Hounsfield unit (H) readings. We made six arbitrary divisions at increments of 7 H ± 3 H, from ≤15 H to ≥ 44 H. The values of the partial curves were then grouped accordingly. The distribution of standard mean values is shown in table 1.

It is not surprising that we found hypodense portions (groups 1–

[1] Abteilung für Neuroradiologie, Kopfklinik der Universität, Würzburg, West Germany. Address reprint requests to M. Ratzka, Josef Schneider Strasse 11, 87 Würzburg, West Germany.

[2] Institut für angewandte Mathematik und Statistik der Universität Würzburg, Am Hubland, 87 Würzburg, West Germany.

AJNR 4:505–508, May/June 1983 0195–6108/83/0403–0505 $00.00

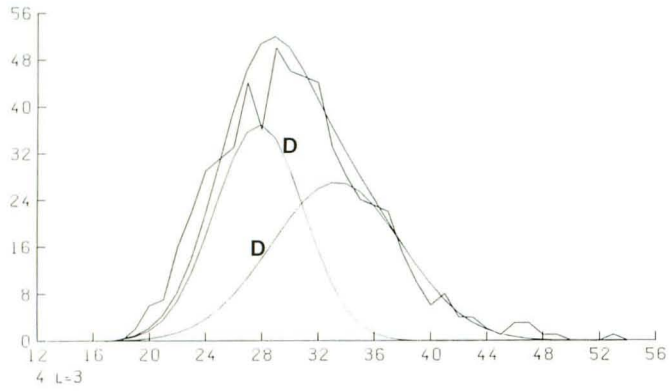

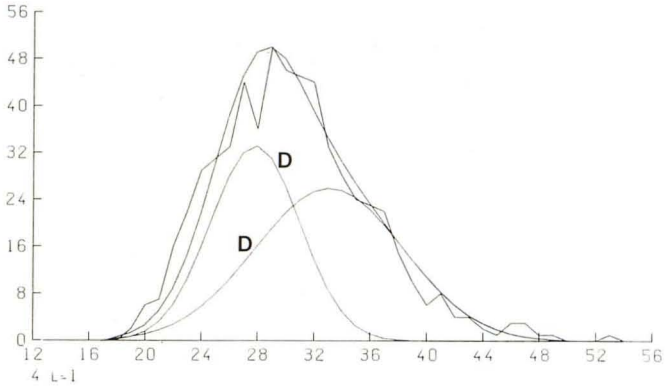

Fig. 1.—Sample of computer-disintegrated histogram. Nearly normal-appearing distribution curves from histogram printouts can be disintegrated to reveal mixed distribution of two tissue components (D). Resulting mean attenuation values are 28 H for white matter and 38 H for gray matter.

3) in all cases except one and isodense portions (group 4) in 38 of the 50 cases. But what is striking is the fact that we found only eight cases of the 50 that did not contain a portion categorized as group 5 or 6, representing material that is hyperdense compared with normal brain tissue. (The partial curves in the lower attenuation value range represent hypodense tumor areas as well as areas of central tumor necrosis, or include areas of edema surrounding tumors. Some general mean values are: perifocal edema, 18–26 H; central tumor necrosis, 19–23 H; and tumor cysts, 6–22 H [1].)

Histograms after Contrast Enhancement of the Tumors

Enhancement was obtained by intravenous application of iodine contrast medium (300 mg I/ml either as a bolus injection of 1 ml solution/kg body weight or as a prolonged bolus of 100 mg solution). Plain scan histograms were compared with those of the contrast medium–enhanced tumors in all cases (fig. 2).

In comparing the mean attenuation values of all the histograms before and after contrast enhancement we found weak or no enhancement (≤5 H) in 20 cases; moderate enhancement (6–10 H) in 20 cases; marked enhancement (11–15 H) in nine cases; and high enhancement (>16 H) in one case. The first group consisted of 13 cases without significant visible enhancement effect and seven cases with marked partial enhancement (visual evaluation). The one case with high enhancement effect was also a partially enhancing tumor.

In comparing the highest Hounsfield number in the tumor histogram before and after contrast medium enhancement we found an increase in Hounsfield units after enhancement. Attenuation values after enhancement were: ≤5 H in 13 cases; 6–10 in 11 cases; 11–15 in 14 cases; 16–20 in eight cases; and >20 in four cases.

In our visual evaluation of the CT pictures before and after contrast enhancement of the tumors we found no significant enhancement in 13 cases, partial enhancement in 32 cases, and nearly total enhancement in five cases.

We also investigated the relations between the partial curves of the tumor histograms before and after contrast enhancement. Concerning the incidence of increase of the mean attenuation values in the partial curves, we found no enhancement effect at all in seven cases; an increase of the mean value (ΔM) of one partial curve (ΔM ≤ 5 H) in eight cases; an increase of the mean value of two partial curves (ΔM ≤ 5 H) in 12 cases; an increase of the mean values of more than two partial curves (ΔM ≤ 5 H) in eight cases; and the emergence of additional partial curves with higher attenuation values (more partial curves after enhancement than in the plain scan histogram) in 15 cases.

TABLE 1: **Mean Attenuation Values (Unenhanced) of Disintegrated Distribution Curve**

No. Cases/Combination of Groups	Group No.					
	1	2	3	4	5	6
1	X	X		X		
1	X	X			X	
2		X	X	X		
5		X		X		
11		X	X	X	X	
8		X	X		X	
1		X	X	X		X
5		X		X	X	
1		X		X	X	X
3			X	X	X	
5			X	X	X	X
3			X	X		X
3			X		X	X
1				X	X	X

Note.—Group values were assigned as follows: group 1, ≤ 15 H; group 2, 16–22 H; group 3, 23–29 H; group 4, 30–36 H; group 5, 37–43 H; group 6, ≥ 44 H.

When we studied the intensity of the contrast enhancement shown by the partial curves by comparing the highest mean attenuation value (peak) of a partial curve before and after contrast medium enhancement we found an increase in the number of peaks with a mean attenuation value ≥44 H in 11 cases (18 before, 29 after enhancement); ≥50 H in 31 cases (three before, 34 after enhancement); and ≥60 H in 11 cases (all after enhancement).

In 32 cases, one or two of the groups with lower attenuation values remained at the same peak—a sign of partial nonenhancement of tissue elements. On the other hand, this effect also helps to prove the validity of the calculation made to separate the diverse tissue elements, because it corresponds entirely with the visual finding of partial enhancement.

In 35 cases comparing the plain scan histograms and the curves after enhancement the number of partial curves corresponds, so the enhancement effect of the diverse fractions can be correlated directly. But in 15 cases we found additional partial curves after enhancement. This phenomenon may be a nonhomogenous contrast enhancement effect on a higher attenuating, apparently ho-

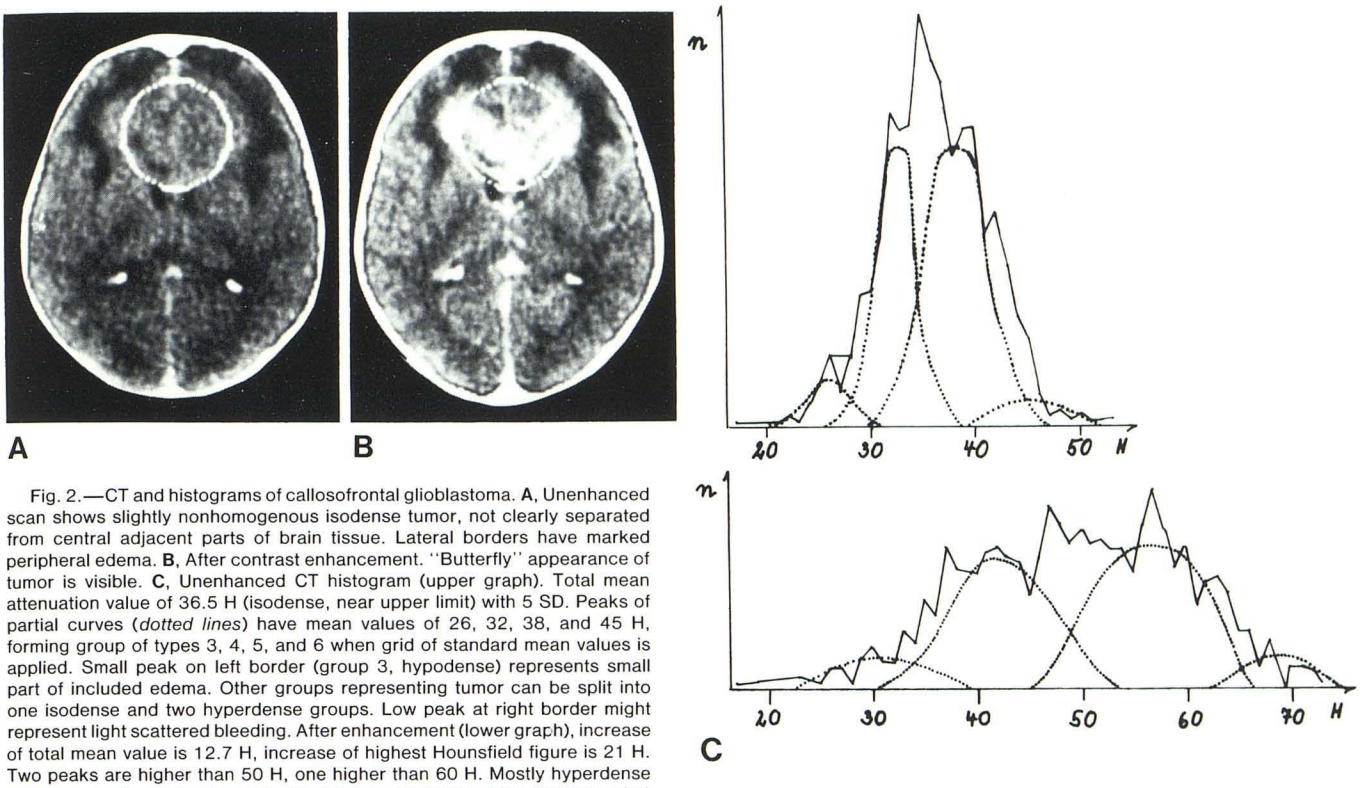

Fig. 2.—CT and histograms of callosofrontal glioblastoma. **A**, Unenhanced scan shows slightly nonhomogenous isodense tumor, not clearly separated from central adjacent parts of brain tissue. Lateral borders have marked peripheral edema. **B**, After contrast enhancement. "Butterfly" appearance of tumor is visible. **C**, Unenhanced CT histogram (upper graph). Total mean attenuation value of 36.5 H (isodense, near upper limit) with 5 SD. Peaks of partial curves (*dotted lines*) have mean values of 26, 32, 38, and 45 H, forming group of types 3, 4, 5, and 6 when grid of standard mean values is applied. Small peak on left border (group 3, hypodense) represents small part of included edema. Other groups representing tumor can be split into one isodense and two hyperdense groups. Low peak at right border might represent light scattered bleeding. After enhancement (lower graph), increase of total mean value is 12.7 H, increase of highest Hounsfield figure is 21 H. Two peaks are higher than 50 H, one higher than 60 H. Mostly hyperdense component after enhancement may be caused by vascular (intravascular) enhancement effect.

mogenous tumor fraction. Or, because it occurs only in the range of the highest mean attenuation values (M > 60 H), it may be the documentation of intravascular contrast enhancement effects.

Discussion

Much has been accomplished to make CT diagnoses as reliable as possible [1, 4–13], and while we agree that nothing demonstrates the significant elements of a CT scan better than the CT picture itself, we nevertheless have to search for new bases from which we can develop new parameters. One way may be the elaboration of statistical data which are inherent in the digital information of the scan pictures.

We have introduced a method to elaborate statistical data from histograms of ROIs of brain tumors. The method is rather elementary as far as the fundamentals are concerned, but the realization and the interpretation of the results are not yet finished. First, it is rather complicated to get more than two partial curves, and some of the findings must be explained by weak points of the arrangements. For instance, the high incidence of hypodense elements is due to the inaccurate placement of the inflexible ROIs, which often include smaller parts of perifocal edema zones. However, in light of other reports [1, 4, 5, 8, 11], the high incidence of isodense or hyperdense areas seems to be a novelty. This phenomenon cannot be explained sufficiently by the influence of partial volume effects in the neighborhood of bony structures. If the histogram curve of an apparently homogenous isodense or hyperdense tumor can be dissected into two curves of normal statistical distribution, the conclusion must be that there do exist different tissue elements mixed up in the sample. This would be a new finding. In the case of glioblastomas or anaplastic gliomas, such hyperdense elements could be scattered punctiform bleedings (which are well known from the gross pathologic anatomy) or very slight calcifications.

Through the culling of partial curves from tumor histograms we have been able to get more information about nonhomogenous tumors and other tissue elements that are not visually apparent. We have found that comparison of partial curves of histograms of unenhanced and enhanced tumors leads to a better quantification of nonhomogenous or latent enhancement reactions. In some cases it is even possible to separate intravascular contrast media.

Further studies need to be in several areas. For instance, the number of the pixels in the partial curves is available, but this has not been a point of investigation yet. With them it will be possible to define the size of the partial curves. In this way the system could be used to detect rather small alterations in the quality and quantity of pathologic findings. This would be useful for very sensitive follow-up studies of tumor patients [14]. The comparison of plain and enhanced scans by this means would also provide a rather accurate estimate of the dimensions of contrast media effects. This might in turn be applicable in the future to the development of such complicated procedures as dynamic contrast studies or blood volume studies. Also, the use of an up-to-date scanning system would eliminate the inaccuracy of the ROI setting and some disturbances caused by partial volume effects and poor density differentiation. The integration of the method into the scanner software program or another on-line system would allow the investigation of greater volumes using this method.

REFERENCES

1. Kazner E, Wende S, Grumme T, Lanksch W, Stochdorph O, eds. *Computed tomography in intracranial tumors*. Berlin: Springer-Verlag, **1982**:18–21, 32, 61

2. Weichselberger K. Über ein graphisches Verfahren zur Trennung von Mischverteilungen und zer Identifikation kupierter Normalverteilungen bei großem Stichprobenumfang. *Metrika* **1961**;4:178–229
3. Knoll F. Zur Großzahlforschung. Über die Zerspaltung einer Mischverteilung in Normalverteilungen. *Archiv Mathematische Wirtschaft Sozialforschung* **1942**;8:36–49
4. Ambrose J. Computerized axial tomography. Part 2: Clinical applications. *Br J Radiol* **1973**;46:1023
5. New PFJ, Scott WR, Davis KR, Taveras JM, Hochberg FH. Computed tomography with the EMI-scanner in the diagnoses of primary and metastatic intracranial neoplasms. *Radiology* **1975**;114:75
6. Gado M, Phelps M, Coleman RE. An extravascular component of contrast enhancement in cranial computed tomography. *Radiology* **1975**;117:589–597
7. Penn RD, Walser R, Kurtz D, Ackerman L. Tumor volume, luxury perfusion and regional blood volume changes in man visualized by subtraction in computerized tomography. *J Neurosurg* **1976**;44:449
8. Grumme T, Steinhoff H. Wende S. Diagnosis of supratentorial tumors with computerized tomography. In: Lanksch W, Kazner E, eds.: *Cranial computerized tomography*. Berlin: Springer-Verlag, **1976**:18, 21, 23
9. Gardeur D, Sablayrolles JL, Klausz R, Metzger K. Histographic studies in computed tomography of contrast enhanced cerebral and orbital tumors. *J Comput Assist Tomogr* **1977**;1:37–41
10. Kramer RA, Yoshikawa M, Scheibe PO, Janetos GP. Statistical profiles in computed tomography. *Radiology* **1977**;125:145–147
11. Steinhoff H, Lanksch W, Kazner E, et al. CT in diagnosis and differential diagnosis of glioblastomas. *Neuroradiology* **1977**;14:193–200
12. Emde M, Braun-Feldweg M, Piepgras U. Die quantitative Bildanalyse im Rahmen der kranialen Computertomographie. *ROFO* **1979**;131:666–669
13. Nadjmi M, Piepgras U, Vogelsang H, eds. *Kranielle Computertomographie*. Stuttgart: Thieme, **1981**:253–263
14. Kretzschmar K, Schicketanz KH. Measurement of the volume and density of intracerebral tumors by CT following therapy. *Neuroradiology* **1982**;23:175–184